

## Development of Tetracycline by Fe<sub>2</sub>O<sub>3</sub> Nanoparticles and Studying Its Activity on Antibiotic-Resistant Bacteria

Wafaa Majeed<sup>1</sup> , Mustafa Hameedi<sup>2</sup> , Maryam O. Abd Alaa<sup>3</sup>

### Abstract

One of the most important modern approaches to preventing antibiotic resistance is the production of antibiotics utilizing nanotechnology. To make nano-antibiotics, Fe<sub>2</sub>O<sub>3</sub> particles were generated using the chemical precipitation approach and combined with Tetracycline using the physical method, utilizing ultrasonic equipment. The TCS nanoparticle dispersion in the tetracycline particle-matrix was found to be stable. The resultant nanocomposites were evaluated using XRD, EDX, and SEM techniques, and their properties were compared to those in the ICDD database [ICDD card no. 0664-33]. The average crystal size of Fe<sub>2</sub>O<sub>3</sub> was 36.75 nm, whereas the average crystal size of Fe<sub>2</sub>O<sub>3</sub>+TCS was 28.10 nm. TCS bound with Fe<sub>2</sub>O<sub>3</sub> was tested for bacterial activity. It was compared to normal tetracycline particles by evaluating the lowest inhibitory concentration of two species of bacteria using an ELISA method. Fe<sub>2</sub>O<sub>3</sub>+TCS NPs had a MIC of 32 µg/ml against Staphylococcus, indicating good bactericidal effectiveness. In comparison, the MIC of standard TCs was 512 µg/ml, showing that the aforesaid chemical was more effective than regular TCs. In comparison to conventional TCs of 512 µg/ml, Fe<sub>2</sub>O<sub>3</sub>+TCS NPs showed a MIC of 128 µg/ml against Pseudomonas aeruginosa. Hemolysis was also performed to test the compound's toxicity (Fe<sub>2</sub>O<sub>3</sub>+TCS NPs). The compounds were found to be safe at all concentrations except 500 µg/ml, according to the results of the experiments.

**Keywords:** Tetracycline, Fe<sub>2</sub>O<sub>3</sub> Nanoparticles, Antibiotic-Resistant

تطوير التتراسيكلين بواسطة جزيئات Fe<sub>2</sub>O<sub>3</sub> النانوية ودراسة نشاطه على البكتيريا المقاومة للمضادات الحيوية

م.م. وفاء مجيد يحيى حسين<sup>1</sup> ، أ.د. مصطفى عبد المجيد حميد<sup>2</sup> ، مريم عمران عبدالله<sup>3</sup>

### المستخلص

تهدف الدراسة الى حد أهم الأساليب الحديثة لمنع مقاومة المضادات الحيوية هو إنتاج المضادات الحيوية باستخدام تقنية النانو. لصنع المضادات الحيوية النانوية ، تم إنشاء جزيئات Fe<sub>2</sub>O<sub>3</sub> باستخدام نهج الترسيب الكيميائي ودمجها مع التتراسيكلين باستخدام الطريقة الفيزيائية باستخدام جهاز الموجات فوق الصوتية. وجد أن تشتت الجسيمات النانوية TCS في مصفوفة جسيمات التتراسيكلين مستقر. تم تقييم المركبات النانوية الناتجة باستخدام تقنيات XRD و EDX و SEM ، وتمت مقارنة خصائصها بتلك الموجودة في قاعدة بيانات ICDD [بطاقة ICDD رقم. 33-0664]. كان متوسط الحجم البلوري لـ Fe<sub>2</sub>O<sub>3</sub> 36.75 نانومتر ، في حين كان متوسط حجم بلورة Fe<sub>2</sub>O<sub>3</sub> + TCS 28.10 نانومتر. تم اختبار TCS المرتبط بـ Fe<sub>2</sub>O<sub>3</sub> من أجل النشاط البكتيري. تمت مقارنته بجزيئات التتراسيكلين العادية من خلال تقييم أقل تركيز مثبط لنوعين من البكتيريا باستخدام طريقة التركيز المثبط الأدنى . يحتوي Fe<sub>2</sub>O<sub>3</sub> + TCS NPs على MIC قدره 32 µg/ml ضد المكورات العنقودية ، مما يشير إلى فعالية جيدة للجراثيم. في المقارنة ، كان MIC لـ TCs القياسية 512 µg/ml ، مما يدل على أن المادة الكيميائية المذكورة كانت أكثر فعالية من المساهمين الأساسيين العاديين. بالمقارنة مع TCs التقليدية من 512 µg/ml ، أظهر Fe<sub>2</sub>O<sub>3</sub> + TCS NPs MIC من 128 µg/ml ضد الزائفة الزنجارية. تم إجراء انحلال الدم أيضًا لاختبار سمية المركب (Fe<sub>2</sub>O<sub>3</sub> + TCS NPs). وجد أن المركبات آمنة في جميع التراكيز ما عدا 500 µg/ml حسب نتائج التجارب.

### Affiliation of Authors

<sup>1,2,3</sup> College of Education for Pure Science, Univ. of Diyala, Iraq, Diyala, 32001

<sup>1</sup> wafa.majeed.yeha@uodiyala.edu.iq

<sup>2</sup> mustafa.hameed@uodiyala.edu.iq

<sup>3</sup> mariamomran1982@uodiyala.edu.iq

### <sup>1</sup> Corresponding Author

### Paper Info.

Published: Jun. 2025

### انتساب الباحثين

<sup>1,2,3</sup> كلية التربية للعلوم الصرفة، جامعة ديالى، العراق، ديالى، 32001

<sup>1</sup> wafa.majeed.yeha@uodiyala.edu.iq

<sup>2</sup> mustafa.hameed@uodiyala.edu.iq

<sup>3</sup> mariamomran1982@uodiyala.edu.iq

### <sup>1</sup> المؤلف المراسل

### معلومات البحث

تاريخ النشر : حزيران 2025

## Introduction

The first tetracycline antibiotics were discovered more than 50 years ago by researchers from many pharmaceutical corporations. The antibiotics chlortetracycline and tetracycline were byproducts of secondary metabolism [1]. As well as being chemically transformed from chlortetracycline in the case of tetracyclines, these compounds were discovered by systematically sampling the fermentation products of spore-forming soil bacteria. They were quickly introduced into clinical practice and, in many cases, agriculture as feedstocks [2]. A tetracyclic system is present in the main structure of the tetracycline antagonist. After chemical alteration in the upper section, the antibiotic's characteristics are mainly preserved. Because it comprises a new divalent metal chelation site required for biological activity, the lower section can be replaced. Tetracyclines work as antibiotics by attaching to the bacterial ribosome and preventing protein translation [3]. Tetracycline has a lot of binding sites on the ribosome, which decreases protein synthesis. Instead of dying, the cell stops growing as a result of this. Tetracycline enters Gram-negative bacteria via transmembrane binding, followed by passive diffusion of the metal-free antibiotic across the cell membrane. Tetracycline resistance developed quickly when it was first used in clinical trials. The horizontal exchange of resistance genes on motile genetic elements such as plasmids and linings resulted in the rapid development of resistance in many bacterial species. Tetracycline resistance, like most antibiotics, can develop through a variety of pathways. These include active tetracycline influx from the cell, ribosome-protecting protein synthesis, decreased drug permeability, target

mutation, and antibiotic enzymatic breakdown. Bivalent metal binding is required for antibiotic transport into the cell and binding to the target as a result of this resistance [2]. Traditional antibiotic compounds cannot penetrate bacterial cell membrane barriers as precisely and steadily as nanoscale antibiotic molecules, alone or in conjunction with NPs. [4]. Due to their distinct physical, chemical, optical, and mechanical properties, inorganic nanoparticles have drawn much attention.  $Fe_2O_3$  nanoparticles have recently attracted much attention since they are non-toxic, inexpensive, versatile, economically stable, and thermally stable. [5]. Recent discoveries in nanotechnology promise to pave the way for new approaches to treating bacterial diseases, synthesizing alternative antimicrobial drugs, preventing biofilm formation, medication delivery, and cell therapy [6].  $Fe_2O_3$  nanoparticles could have a lot of advantages. Antibacterial activity refers to chemicals that are confined and kill or limit the growth of bacteria without causing harm to the surrounding tissues. Chemically modified natural chemicals make up the majority of today's antibacterial agents [7]. Forced hydrolysis, hydrothermal technology, micro-emulsion technique, sol-gel process, mold-assisted synthesis method, solid vapor growth technique, surface-assisted pyrolysis method, and pyrolysis technique are some of the ways used to make  $-Fe_2O_3$  nanoparticles [8, 9]. This development bodes well for the development of subsequent tetracyclines .

## Items of Research

Spain,  $Fe(NO_3)_2 \cdot 9H_2O$  99.99 Ethylene Glycol 98% INDIA, NaOH 97% INDIA, Hydrochloric

Acid 99% INDIA, Samarra Tetracycline 99.9% Pharmaceutical Company Iraq, Nutrient agar & Muller Bacterial isolates (*Pseudomonas aeruginosa* and *Staphylococcus aureus*) were taken from Baquba Teaching Hospital in Iraq and identified with Hinton broth from HIMEDLA (INDIA).

### Synthesis of Fe<sub>2</sub>O<sub>3</sub> Nanoparticles

Attended in a solution with a concentration of 0.25 M. Fe (NO)<sub>3</sub> is prepared by dissolving 3.7 gm in 50 ml ethylene glycol at 50°C with continuous stirring using a magnetic stirrer and adding the prepared NaOH with a concentration of 0.5 M by dissolving 1.6 gm in 50 ml ionic water by distillation and adjusting the PH to 7 where a gel is formed and then left for 5 days and then dried in a hot air oven at 100°C for 5 hours and then burned.

### Synergistic TCS with Fe<sub>2</sub>O<sub>3</sub> Nanoparticles

0.4 gm Fe<sub>2</sub>O<sub>3</sub> NPs were dissolved in 100 ml of deionized water. Mix 2 gm of TCs with 100 ml of deionized water, then add a solution of NPs Fe<sub>2</sub>O<sub>3</sub> made by mixing 0.5 gm with 100 ml of deionized water, stir for two hours at room temperature, then place it in the ultrasonic machine for three hours, and finally dry it at 45 °C.

### Minimal Inhibitory Concentration for TCs loaded with Fe<sub>2</sub>O<sub>3</sub> NPs

The antagonist (TCs loaded with Fe<sub>2</sub>O<sub>3</sub> NPs) was added in varied amounts from their prepared safe solutions, and then (100 µL) of deionized water was transferred to the plate pits. These antagonist concentrations ranged from (32 - 64 - 128 - 256 - 512-1024 µg/ml). Using a polystyrene plate with 96 holes and (100 µL) of the antibody dispersed in the holes with a maximum concentration of 1024

µg/ml, each bacterial isolate was separated into three duplicates, except the pits containing the control, which included water and cultivated bacteria. Shifts were made by moving (100 µL) of the 1024-concentrated counter-pit to the following hole. Moving from one hole to the next went well. The bacteria were disseminated in (100 µL) for each hole in the plate after we withdrew (100 µL) when we reached the last one. An ELISA reader operating at 630 nanometers was used to monitor the plate after it had been coated and incubated at 37 degrees Celsius [10,11].

### Hemolysis assay for TCs loaded with Fe<sub>2</sub>O<sub>3</sub> NPs

The hemolysis test was performed to screen for nano-antibiotics at different concentrations (32, 64, 128, 500 µg/ml) to find poisonous or harmful substances. The blood sample was retrieved from the lab and deposited in an (EDTA) tube, then tested on a slide and inspected under a microscope at a magnification of (100), confirming that the person's blood was healthy and free of illnesses, with no platelet breakage. The method was used to determine the cytotoxicity of the chemical substances employed [12]. The blood cells and plasma were separated using a (EDTA) tube and a (Universal Centrifuge) for 10 minutes. After removing the plasma layer from the cells, the cells were repeatedly rinsed with PBS, each time adding 1ML of PBS, and centrifuged for 10 minutes. After two minutes, the cells were withdrawn from the PBS. The blood cell suspension was made by mixing (1ML) with (9ML) PBS after the cells had been washed numerous times. In each tube with a volume of (1200 µL), the antagonist is added at different concentrations, and (300 µL) of the cell suspension is added to the final volume (1.5 ml) and incubated in the incubator for two hours, then

separated by a centrifuge device at a rate of 1000 cycles/min for five minutes. The difference in hemolysis was then measured using the Heh control settings (test tube containing blood and deionized water only, test tube containing blood and PBS). If the blood components are combined after centrifugation, the (+) option shows the compound's toxicity. The (-) option shows that following centrifugation, the blood components were not mixed, indicating that the substance was not hazardous.

**Results and discussion**

**Characterization by X-ray diffraction for TCs loaded with Fe<sub>2</sub>O<sub>3</sub> NPs**

Using the International Center for XDR Database (ICDD), the X-ray spectra of Fe<sub>2</sub>O<sub>3</sub> were compared to the material's standard range in Figure (1) (Card no. 33-0664). The average size of the crystals was (36.75 nm). This is supported by the literature [13,14]. The mean crystal size was 28.10 nm, as shown in Figure (2), and the XRD and synergistic TCS spectra were matched to Fe<sub>2</sub>O<sub>3</sub>.

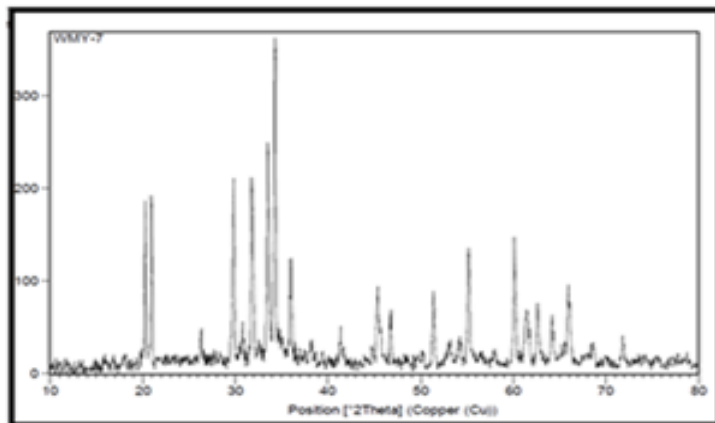


**Figure (1): X- ray diffraction spectrum for Fe<sub>2</sub>O<sub>3</sub>**

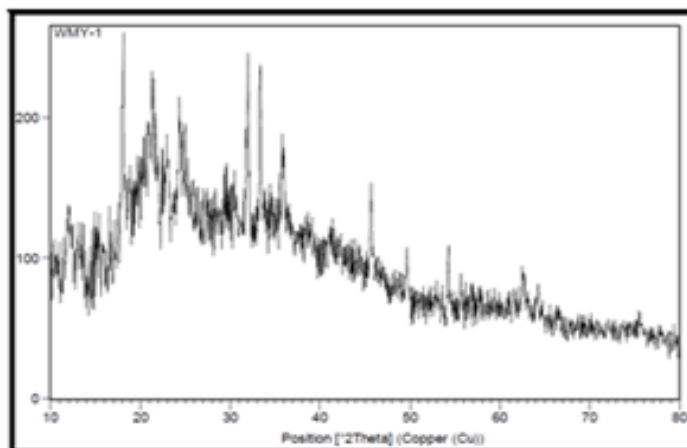


**Figure (2): X- ray diffraction spectrum for synergistic TCs with Fe<sub>2</sub>O<sub>3</sub>**

**Characterization by energy-dispersive X-rays for TCs loaded with Fe<sub>2</sub>O<sub>3</sub> NPs**

The percentage of components present in Fe<sub>2</sub>O<sub>3</sub>

NPs was ascertained using energy-dispersive X ray, as depicted in Figure (3). The data's iron content (64.5%) and oxygen content (35.5%) suggested the presence of a high-purity iron oxide

nanomaterial. Energy-dispersive X-ray analysis of the TCs loaded with Fe<sub>2</sub>O<sub>3</sub> NPs, as shown in Figure (4), indicated substantial concentrations of

carbon (60.6%), iron (13.5%), oxygen (22.1%), and nitrogen (3.8%), as well as pure Fe<sub>2</sub>O<sub>3</sub> NPs.

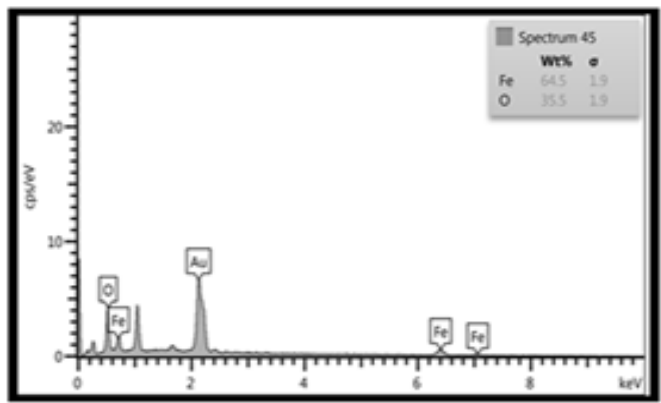


Figure (3): EDX spectrum of Fe<sub>2</sub>O<sub>3</sub>

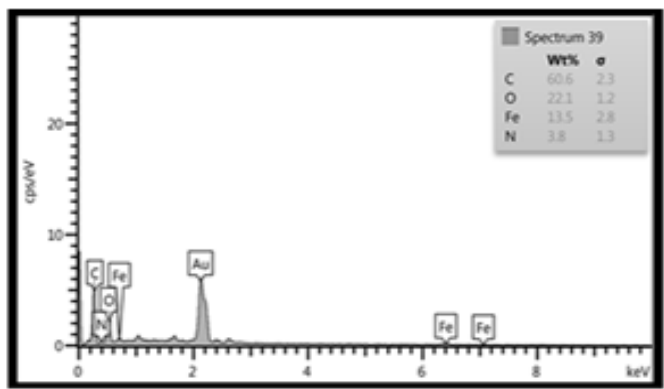
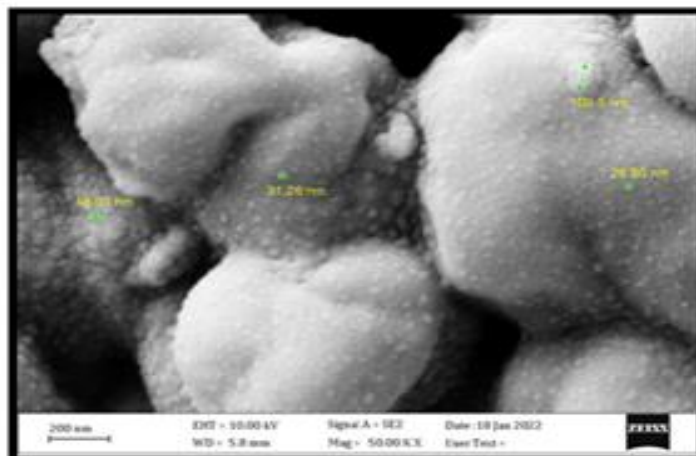


Figure (4): EDX spectrum of TCs with Fe<sub>2</sub>O<sub>3</sub>

**Characterization by scanning electron microscope**

The morphological and structural makeup of Fe<sub>2</sub>O<sub>3</sub> NPs was examined using an SEM scanning electron microscope. As illustrated in Figure 5, the nanoscale range was used to generate the nanoparticles, and SEM scans showed that some of the particles separated well from one another. Electrostatic effects caused most of them to be present at once in lumpy form. The average diameter of these nanoparticles is 53.39 nm, and their behavior is consistent with past studies of

nanoparticle agglomeration. Figure 6 shows that the ratio of morphological and structural TCs loaded with NPs Fe<sub>2</sub>O<sub>3</sub> caused the nanoparticles to be produced in the nanoscale range. Some of the nanoparticles were well segregated from one another, according to SEM images. Most of them were present but agglomerated due to electrostatic forces simultaneously, consistent with earlier discoveries about nanoparticle agglomeration. The average diameter of these nanoparticles is 62.796 nm.



**Figure (5): SEM image of Fe<sub>2</sub>O<sub>3</sub>**

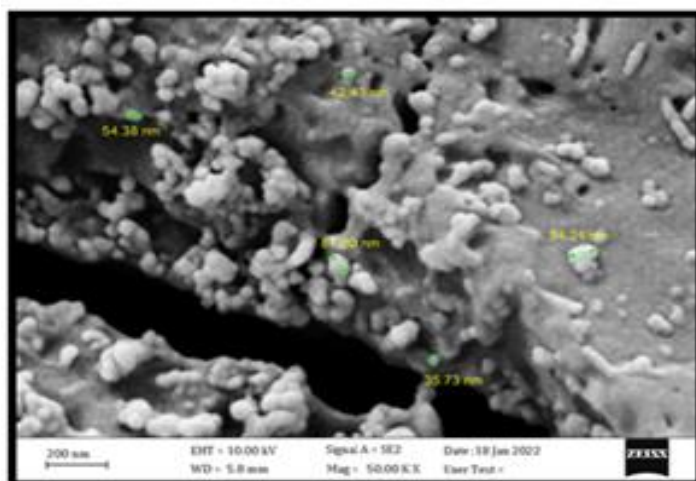


**Figure (6): SEM image of TCs with Fe<sub>2</sub>O<sub>3</sub> NPs**

### **Isolating Bacteria for *Pseudomonas aeruginosa* and *Staphylococcus aureus***

The isolates used in this investigation were from Baquba Teaching Hospital's clinical and laboratory sources. Using vitek® 2, antibiotic resistance was assessed. According to the findings, *Pseudomonas aeruginosa*, the first isolate, was resistant to several different antibiotics, including Cefotaxime, Amikacin, Gentamicin, Ticarcillin-Clavulanate, Piperacillin, Cefepime, Ciprofloxacin, Tobramycin, Ceftazidime, Levofloxacin, Polymyxin, and Meropenem. The second isolate was insensitive to the antibiotics Levocin, Staphylacin, Benzylcom, Gentamicin,

Tobramycin, Linezolid, Teicoplanin, Tetracycline, and Tigecycline.

### **Determination of Minimal Inhibitory Concentration**

The lowest inhibitory concentration of (TCs, TCs + Fe<sub>2</sub>O<sub>3</sub> NPs) compounds was determined using resistant bacterial isolates. The multiplicative serial concentration approach (32-64-128-256-512-1024 μg/ml) was used to determine the MIC with Middle Mueller Hinton Broth. Table 1 shows the results. The minimum inhibitory concentration of TCs loaded with Fe<sub>2</sub>O<sub>3</sub> against *Pseudomonas aeruginosa* was 128 μg/ml, whereas the standard

base contributions were 512 µg/ml TCs, showing that the aforesaid compound has a higher activity than the standard TCs. The MIC of TCs loaded with Fe<sub>2</sub>O<sub>3</sub> against Staphylococcus aureus was 32

µg/ml, while the MIC of standard TCs was 512 µg/ml, showing that the aforesaid compounds were more effective than the standard components.

**Table (1) Minimal Inhibitory Concentration of (TCs, TCs loaded with Fe<sub>2</sub>O<sub>3</sub>) [18]**

compounds	Pseudomonas aeruginosa MIC µg/ml	Staphylococcus aureus MIC µg /ml
TCs	512	512
TCs + Fe <sub>2</sub> O <sub>3</sub>	128	32

**Determination Hemolysis assay**

The cytotoxicity of the compound (TCs loaded with Fe<sub>2</sub>O<sub>3</sub> NPs) was investigated, and the results

showed that the compound was safe (non-toxic) at all concentrations except 500µg / mL, which showed a toxic effect in the form of fractured platelets, as shown in Table (2) and Figure (7).

**Table (2) is used to evaluate the toxicity of a chemical (TCs + Fe<sub>2</sub>O<sub>3</sub> NPs)[18]**

TCs + Fe <sub>2</sub> O <sub>3</sub> NPs	32	-
	64	-
	128	-
	500	+

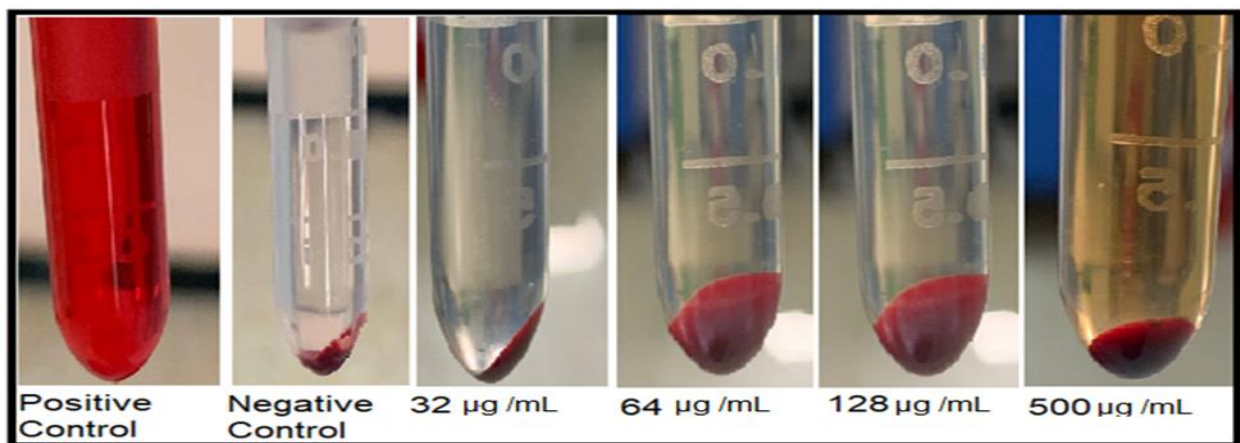


**Figure (7): Hemolysis test for anti- TCs loaded with Fe<sub>2</sub>O<sub>3</sub> NPs**

The iron oxide complex NPs have an acceptable crystal structure and a virtually homogeneous interaction with Fe<sub>2</sub>O<sub>3</sub>+TCS in the nano size range. Because some bacteria have high resistance, shrinking the NPs to increase the metal oxide's toxicity is a good idea. However, nanoparticles

with a larger number of reactive groups and a larger surface area on the active sites of ROS formation, resulting in oxidative stress, could be a good candidate for explaining why the high efficacy [15]. Several studies show that metal oxide compounds' antibacterial action in the

aqueous system is mostly due to the ions' high solubility, which has an influence on cellular function due to the buildup of NPs in an aqueous medium [16]. However, at higher concentrations of NPs, the metallic ionic form, which is described as a mechanical type Trojan that lets antibiotics like TCS to enter and becomes more potent after interacting with  $\text{Fe}_2\text{O}_3$ , can be more Cytotoxic [17].

### Conclusions

Based on our findings, we can conclude that  $\text{Fe}_2\text{O}_3$ +TCS NPs binding is a good choice in antibiotic development and opens up a new way of using nanotechnology to make drugs that have the ability to inhibit growth against resistant bacteria, but at higher concentrations of MIC, it is assumed that it can adapt with Fe ions that can be used as an energy source in the metabolic pathway. Combining antibiotics with the bactericidal action of these NPs against suspended bacteria at a certain concentration can be a suitable alternative. Furthermore, these nanoparticles have no toxicity.

### References

- [1] Ye, J., Du, Y., Wang, L., Qian, J., Chen, J., Wu, Q., & Hu, X. (2017). Toxin release of cyanobacterium *Microcystis aeruginosa* after exposure to typical tetracycline antibiotic contaminants. *Toxins*, 9(2), 53.
- [2] Roberts, M. C. (2019). Tetracyclines: mode of action and their bacterial mechanisms of resistance. *Bacterial Resistance to Antibiotics—From Molecules to Man*, 101-124.
- [3] Aleksandrov, A., & Simonson, T. (2008). Molecular dynamics simulations of the 30S ribosomal subunit reveal a preferred tetracycline binding site. *Journal of the American Chemical Society*, 130(4), 1114-1115.
- [4] Jijie, R., Barras, A., Teodorescu, F., Boukherroub, R., & Szunerits, S. (2017). Advancements on the molecular design of nanoantibiotics: current level of development and future challenges. *Molecular Systems Design & Engineering*, 2(4), 349-369.
- [5] Long, N. V., Yang, Y., Teranishi, T., Thi, C. M., Cao, Y., & Nogami, M. (2015). Synthesis and magnetism of hierarchical iron oxide particles. *Materials & Design*, 86, 797-808.
- [6] Weissleder, R., Nahrendorf, M., & Pittet, M. J. (2014). Imaging macrophages with nanoparticles. *Nature materials*, 13(2), 125-138.
- [7] Sarkar, A., & Sil, P. C. (2014). Iron oxide nanoparticles mediated cytotoxicity via PI3K/AKT pathway: role of quercetin. *Food and Chemical Toxicology*, 71, 106-115.
- [8] Li, L., Wang, B., & Chu, Y. (2015). A novel approach to synthesizing hollow  $\alpha\text{-Fe}_2\text{O}_3$  spheres via hydrothermal treatment. *Research on Chemical Intermediates*, 41(5), 3003-3010.
- [9] Kloust, H., Zierold, R., Merkl, J. P., Schmidtke, C., Feld, A., Pösel, E., ... & Weller, H. (2015). Synthesis of iron oxide nanorods using a template-mediated approach. *Chemistry of Materials*, 27(14), 4914-4917.
- [10] Wayne, P. A. (2011). Clinical and Laboratory Standards Institute. Performance standards for antimicrobial susceptibility testing.
- [11] Tang, J., Kang, M., Chen, H., Shi, X., Zhou, R., Chen, J., & Du, Y. (2011). The staphylococcal nuclease prevents biofilm formation in *Staphylococcus aureus* and other biofilm-forming bacteria. *Science China Life Sciences*, 54(9), 863-869.

- [12] Wayne, P. A. (2011). Clinical and Laboratory Standards Institute. Performance standards for antimicrobial susceptibility testing.
- [13] Lassoued, A., Dkhil, B., Gadri, A., & Ammar, S. (2017). Control of the shape and size of iron oxide ( $\alpha$ -Fe<sub>2</sub>O<sub>3</sub>) nanoparticles synthesized through the chemical precipitation method. *Results in physics*, 7, 3007-3015.
- [14] Upadhyay, S., Parekh, K., & Pandey, B. (2016). Influence of crystallite size on the magnetic properties of Fe<sub>3</sub>O<sub>4</sub> nanoparticles. *Journal of Alloys and Compounds*, 678, 478-485.
- [15] Shahbazi, E., Morshedzadeh, F., & Zaeifi, D. (2019). Bacteriostatic potency of Fe<sub>2</sub>O<sub>3</sub> against *Enterococcus faecalis* in synergy with antibiotics by the DDST method. *Avicenna Journal of Medical Biotechnology*, 11(2), 176.
- [16] Wu, B., Huang, R., Sahu, M., Feng, X., Biswas, P., & Tang, Y. J. (2010). Bacterial responses to Cu-doped TiO<sub>2</sub> nanoparticles. *Science of the total environment*, 408(7), 1755-1758.
- [17] Limbach, L. K., Wick, P., Manser, P., Grass, R. N., Bruinink, A., & Stark, W. J. (2007). Exposure of engineered nanoparticles to human lung epithelial cells: influence of chemical composition and catalytic activity on oxidative stress. *Environmental science & technology*, 41(11), 4158-4163.
- [18] CLSI. Clinical and Laboratory Standards Institute. (2016). standards for antimicrobial susceptibility Testing; Twenty-Second informational supplement. CLSI Document M100-S26. Wayne, PA: Clinical and Laboratory Standards Institute